Biotechnology Reports 30 (2021) e00614

Contents lists available at ScienceDirect

Biotechnology Reports

journal homepage: www.elsevier.com/locate/btre

Agricultural waste of sugarcane bagasse as efficient adsorbent for lead and nickel removal from untreated wastewater: Biosorption, equilibrium isotherms, kinetics and desorption studies

Blessing Amaka Ezeonuegbu[a,*], Dauda Abdulahi Machido[a], Clement M.Z. Whong[a], Wisdom Sohunago Japhet[b], Athanasios Alexiou[c], Sara T. Elazab[d], Naeem Qusty[e], Clement Ameh Yaro[f], Gaber El-Saber Batiha[g]

[a] *Department of Microbiology, Ahmadu Bello University, Zaria, Nigeria*
[b] *Department of Botany, Ahmadu Bello University, Zaria, Nigeria*
[c] *Novel Global Community Educational Foundation, Australia and AFNP Med, Austria*
[d] *Department of Pharmacy, Faculty of Veterinary Medicine, Mansoura University, Mansoura 33516, Egypt*
[e] *Medical Laboratories Department, Faculty of Applied Medical Sciences, Umm Al-Qura University, Mecca, Saudi Arabia*
[f] *Department of Animal and Environmental Biology, University of Uyo, Akwa Ibom State, Nigeria*
[g] *Department of Pharmacology and Therapeutics, Faculty of Veterinary Medicine, Damanhour University, Damanhour 22511, AlBeheira, Egypt*

ARTICLE INFO

Article history:
Received 10 July 2020
Received in revised form 18 March 2021
Accepted 19 March 2021

Keywords:
Biosorption
Sugarcane bagasse
Lead ions
Nickel ions
Isotherm and kinetic models

ABSTRACT

The aim of this study was to evaluate the removal of Pb (II) and Ni (II) from untreated waste water using sugarcane bagasse and possible desorption of the metal ions from the adsorbent for effective re-use. The effects of pH (4-6), temperature (30–70 °C), contact time (30–150 min) and adsorbent dosage (0.3–0.7 g) were examined. Optimum conditions for the removal efficiencies of Pb (89.31 %) and Ni (96.33 %) were pH, 6.0; temperature, 30 °C; contact time, 90 min. and adsorbent dosage, 0.5 g. The maximum monolayer adsorption capacities of Pb (II) and Ni (II) were 1.61 mg/g and 123.46 mg/g respectively, by fitting the equilibrium data to the Langmuir isotherm model. Freundlich isotherm and pseudo second order kinetic models were best fitted for Pb (II) and Ni (II) uptake. Desorption of the metal ions from the metal-loaded bagasse was best performed by HNO_3 with removal efficiency of 85.2 %. Therefore, sugarcane bagasse has a high potential for removal of heavy metals from waste water and can be re-used at any time after desorption without losing its efficiency.

1. Introduction

Environmental pollution through industrialization and the excessive use of chemicals all over the world has led to the release of toxic pollutants including heavy metals. The presence of heavy metals in the environment is a serious problem to be addressed in the world today due to their high toxicity, mobility in the environment and non-biodegradability [1,2]. Heavy metals which originates from the mining, electroplating, refinery and other industrial wastewater can cause potential damage to the ecosystem, human and animal health even at low concentration [3–5].

Disposal of wastewater containing heavy metals (lead, nickel, cadmium, chromium, arsenic, etc.) into terrestrial and aquatic environment, can cause deterioration in water quality and toxicity to human health. At high concentrations, most heavy metal ions can damage cell membrane, alter enzyme activities, disrupt cellular function, and have been linked to birth defects, cancer, skin lesions, growth retardation leading to disabilities, kidney and liver damage and other health problems [6,7].

Globally, lead consumption has been on the on the increase due to the increase demand for cars and power assisted machines. Lead which exist in several oxidation states (0, +1, +2 and +4), is known for its toxicity and environmental impact. It can be accumulated and adsorbed by the body through inhalation, ingestion, skin contact and transfer through the placenta [1,3]. Long-term exposure of lead to children, not only impacts their biological systems, but also has long-term effects, such as damage to central nervous system and chronic respiratory diseases [8–10].

* Corresponding author.
E-mail addresses: amakaezeonu@gmail.com (B.A. Ezeonuegbu), Machaisha100@gmail.com (D.A. Machido), clementwhong@gmail.com (C.M.Z. Whong), wjaphetspessece@gmail.com (W.S. Japhet), alextha@yahoo.gr (A. Alexiou), Sara.taha@ymail.com (S.T. Elazab), nfqusty@uqu.edu.sa (N. Qusty), yaro.ca@uniuyo.edu.ng (C.A. Yaro).

https://doi.org/10.1016/j.btre.2021.e00614

Nickel is a lustrous, silvery, non-biodegradable toxic metal with atomic number of 28. Uptake of high doses of nickel can cause adverse health effects such as birth defect, cancer, respiratory failure, hepatitis, skin rashes, kidney impairment, and diarrhea [11,12].

Efforts have been made by industries (refinery, mining, tannery, electroplating, fertilizers, textiles, dyes, etc.) for the removal of heavy metals from wastewater through conventional methods (membrane filtration; solvent extraction, ion exchange, reverse osmosis, oxidation, chemical precipitation, etc.). However, these methods have many shortcomings of generation of toxic chemical sludge, incomplete metal removal, low efficiency, requirement of high energy and high reagent [13–15]. Hence, new cost effective, safe and economic tools are recommended to reduce the limitations of the conventional methods.

Biosorption is an alternative, favourable and effective tool highly recommended for the removal of heavy metal ions from waste water because of its many advantages of low operation cost, eco-friendly, minimal or no toxic sludge generation, short operating time, easy to prepare, no supplementary nutrient required, possibility of metal recovery and availability [13,14]. Numerous biomass-based adsorbents from biological (fungi, algae, yeast and bacteria) and agricultural origin (rice husk, saw dust, banana peels, corn cob, orange peel, sawdust, sugarcane bagasse, etc.), have been used as adsorbent for heavy metal removal from aqueous solutions with promising results [5,16,17].

Sugarcane (*Saccharum officinarum*) is a widely cultivated tropical plant species in some part of the world (Brazil, India, China, Mexico, South Africa, etc.) which makes up a large proportion of the sugar industries in the world [61]. The composition of sugarcane bagasse is found to consist of about 42 % cellulose, 25 % hemicellulose, and 20 % lignin [10].

It is considered one of the underutilized agricultural wastes compared to other numerous biomass-based adsorbent which have received much attention. In northern part of Nigeria, West Africa, many farmers cultivate sugarcanes as means of livelihood. These sugarcanes are sold to sugar refinery or individuals in communities, markets, villages and to other parts of the country. The bagasse from these canes after chewed or refined are usually thrown away as waste, littering the environment. Through this study, this “waste” was channeled into the useful purpose of biosorption due to its availability and low cost.

The aim of this study was to assess the efficiency of sugarcane bagasse (SCB) for the removal of Pb (II) and Ni (II) from untreated refinery waste water. Therefore, the experiment was performed in batch system and the effect of biosorption factors, equilibrium isotherms, adsorption kinetics and desorption of metal-loaded SCB were investigated.

2. Materials and methods

2.1. Materials and chemicals

All materials and reagents used were of commercial grade. The chemicals used in this study which include nitric acid (HNO_3), sodium hydroxide (NaOH), and hydrochloric acid (HCl) were analytical grade chemicals purchased from Aladdin (Shanghai, China). Milli Q water was used for standardization and preparation of all samples to avoid any interference of other ions.

2.2. Collection of untreated waste water

Samples of untreated effluent were collected from untreated waste water channel of Kaduna Refinery and Petrochemical Company (KRPC), Kaduna State Nigeria. The samples were collected in ten-litre plastic bottles and transported to the laboratory for heavy metal analysis and biosorption studies. The pH and temperature of the effluent were determined at the point of collection.

2.3. Physicochemical and heavy metal analysis

The physicochemical properties of the effluent which include pH, temperature, turbidity, dissolved oxygen, Biological Oxygen Demand, Chemical Oxygen Demand, electrical conductivity, oil and grease, sulphate and phosphate were determined. The concentrations of heavy metals (lead and nickel) in the samples were analyzed using atomic absorption spectrophotometer (AAS).

2.4. Preparation of adsorbent

Sugar cane bagasse (SCB) was collected from several sugarcane vendors in Samaru village, Zaria, Kaduna State, Nigeria. The bagasse was soaked and washed with distilled water, oven dried at 40 °C for 24 h and crushed to a particle size of 0.1 to 0.2 mm [18]. The crushed SCB was transferred into polythene bags, sealed and stored for later use.

2.5. Adsorption studies

2.5.1. Effects of optimization conditions for adsorption

The effects of experimental parameters such as pH, temperature, contact time and adsorbent dosage on adsorption of heavy metals by SCB were investigated. The effect of pH was conducted at pH 4, 5, 6, 7 and 8 by adjusting the untreated effluent using 0.1 N HCl and 0.1 N NaOH solutions. The effect of temperature was conduct at 30, 40, 40, 60 and 70 °C using water bath shaker. The effect of contact time was performed at 30, 60, 90, 120 and 150 min, while the effect of adsorbent dosage was carried out using 0.3, 0.4, 0.5, 0.6 and 0.7 g of adsorbent.

2.5.2. Adsorption experiment

The adsorption experiments were conducted by shaking 0.5 g of SCB with 50 ml of untreated effluent contained in 250 ml conical flasks at 150 rpm. After attaining equilibrium, the samples were separated using filter paper. The concentration of heavy metals in the filtrate was measured using Atomic Absorption Spectrometer (AAS). All experiments were carried out in triplicates. The removal efficiency and quantity of metals adsorbed were calculated using Eqs. (1) and (2) respectively [19].

$$Metal\,removal\,efficiency\,(\%) = \frac{C_i - C_f}{C_i} \times 100 \tag{1}$$

$$Quantity\,of\,metal\,ion\,adsorbed\,(mg/g) = (\frac{C_i - C_f}{m}) \times V \tag{2}$$

Ci and Cf are the initial and final concentrations of metal ions (mg/L), M is the mass of adsorbent (g) and V is the volume of metal ion solution (L).

2.6. Characterization of adsorbent (FTIR and SEM)

The major functional groups on the surface of the SCB before and after metal uptake were identified using Fourier Transform Infrared (FTIR) Spectrophotometer (8400 CE, Shimadzu, Japan). The surface morphology of the SCB before and after uptake were studied using Scanning Electron Microscopy (Thermo Scientific Quanta 650).

Table 1
Physicochemical properties of untreated refinery wastewater.

Parameter	Value (Mean ± SD)	Recommended limit (FMENV)
pH	8.2 ± 0.32	6.0–9.0
Temperature (°C)	26.3 ± 2.31	40
Turbidity (NTU)	433 ± 1.98	5.0
Dissolved oxygen (mg/L)	2.18 ± 0.05	10
Biological Oxygen Demand (mg/L)	145.3 ± 0.11	10
Chemical Oxygen Demand (mg/L)	166.7 ± 20.82	10
Electrical Conductivity (µs/cm)	895.3 ± 2.52	400
Sulphate (mg/L)	72.40 ± 0.57	50
Phosphate (mg/L)	63.20 ± 0.57	5
Oil and Grease (mg/L)	1025 ± 5.00	10
Nitrate (mg/L)	92.5 ± 0.71	10
Lead (mg/L)	0.80 ± 4.05	0.005
Nickel (mg/L)	39.4 ± 1.44	0.07

Keys: *All the values are expressed as Mean ± SD, °C = degree centigrade; NTU = Nephleometric Turbidity Units; mg/L = milligram per litre; µs/cm = micro siemens per centimeter; SD = Standard deviation; FMENV = Federal Ministry of environment Nigeria.

2.7. Equilibrium adsorption isotherm models

Langmuir, Freundlich and Temkin isotherm models were used for fitting the experimental data obtained.

2.7.1. Langmuir isotherm model

Langmuir isotherm is based on the assumptions that adsorption occurs on a homogeneous surface and each adsorption site can hold one metal ion at a time [20,21]. The linearized form of Langmuir isotherm is given in Eq. (3):

$$\frac{C_e}{q_e} = \frac{1}{K_l q_{max}} + \frac{C_e}{q_{max}} \tag{3}$$

Where C_e (mg/L) is equilibrium concentration of the metal ion, q_e is the mass of metal ions adsorbed per mass of adsorbent (mg/g), q_{max} is the maximum monolayer capacity of adsorption (mg/g) and K_L is Langmuir constant. The experimental data were fitted into the above equation by plotting $\frac{C_e}{q_e}$ against C_e. The values of q_{max} and K_L were determined from the slope and intercept respectively.

To determine the viability of the sorption process, a separation factor, R_L (Eq. 4) was used as an indicator of the nature of the sorption process [21].

$$R_L = \frac{1}{1 + K_L C_1} \tag{4}$$

Where C_1 is the initial metal concentration (mg/L); K_L is the Langmuir constant. The favourability of the Langmuir model is such that where R_L <1, Langmuir model is unfavourable; if $R_L = 1$, Langmuir model is linear; if R_L <1 Langmuir model is favourable.

2.7.2. Freundlich isotherm model

Freundlich isotherm is based on the assumption that adsorption occurs on a heterogeneous surface with various adsorption sites which can hold more than one metal ion at a time. [21,22].The linearized Freundlich isotherm is illustrated in Eq. (5):

$$logq_e = logK_F + \frac{1}{n} logC_e \tag{5}$$

Where q_e (mg/g) is the amount of metal ions adsorbed onto the adsorbent at equilibrium, C_e (mg/L) is the heavy metal ions concentration in the solution at equilibrium, K_F and n are Freundlich constants determined from the slope and intercept respectively. The favourability of Freundlich model was determined by n. values of n in the range of 1–10 represent favourable adsorption, while n <1 represent unfavourable adsorption [23].

2.7.3. Temkin isotherm model

The Temkin isotherm model assumes an equal distribution of binding energies over a number of adsorption sites [21,24,25]. The linear form of Temkin isotherm is represented by the Eq. (6):

$$q_e = BLnA + \mathrm{BLn}C_e \tag{6}$$

Where B= $\frac{RT}{b_T}$ with R, the universal gas constant (8.314 kg mol^{-1} K^{-1}) and T as the absolute temperature in Kelvin. q_e (mg/g) is the amount of metal ions adsorbed onto the adsorbent at equilibrium The Temkin parameter A and B are the equilibrium binding energy and heat of sorption respectively.

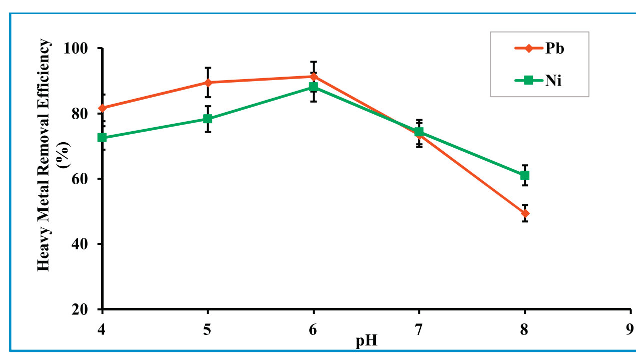

(a): Effect of pH on heavy metal removal by SCB

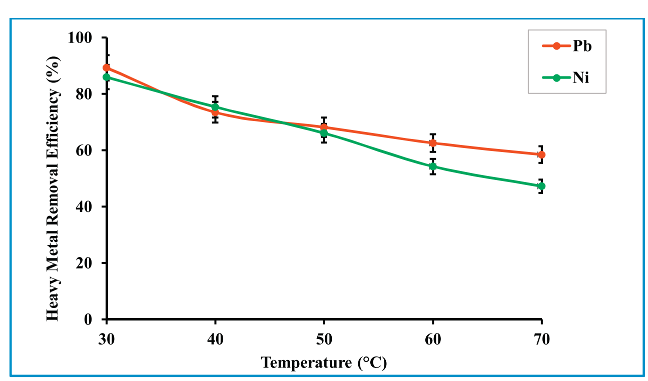

(b): Effect of temperature on heavy metal removal by SCB

Fig. 1. Effect of pH and Temperature on adsorption of lead and nickel.
(a): Effect of contact time on heavy metal removal by SCB.
(b): Effect of adsorbent dosage on heavy metal removal by SCB.

2.8. Adsorption kinetic models

In order to investigate the rate and mechanism of the metal uptake, Pseudo-first order, pseudo-second order and Elovich kinetic models were used to fit the data [26,27].

2.8.1. Pseudo-first order kinetic model

This kinetic model assumes that metal ion binds only to one sorption site on the sorbent surface [23,27]. The pseudo-first order rate equation is expressed in Eq. (7).

$$log(q_e - q_t) = logq_e - \frac{K_1}{2.303}t \tag{7}$$

Where q_e and q_t =Amounts of metal ions (mg/g) adsorbed at equilibrium and at time t respectively, and K_1 = the first-order rate constant (min-1). The value of K_1 was calculated from the slope of the plot of log $(q_e - q_t)$ versus t.

2.8.2. Pseudo-second order kinetic model

The pseudo second order model is based on the assumption that chemical reactions occur between the metal ions and the adsorbent which result in the formation of strong covalent bond [28]. Pseudo-second-order kinetic model is represented by Eq. (8):

$$\frac{t}{q_t} = \frac{1}{K_2 q_e^2 q_2} + \frac{1}{q_2 t} \tag{8}$$

Where q_2 is the maximum adsorption capacity (mg g^{-1}) for the pseudo-second order adsorption and K_2 is the equilibrium rate constant for the pseudo-second order adsorption (g mg^{-1} min^{-1}). The values of K_2 and q_2 was calculated from the plot of t/q_2 versus t.

2.8.3. Elovich kinetic model

Elovich kinetic model assumes that the active sites present on the adsorbent surface are heterogeneous in nature with different activation energy. [24,29]. Elovich kinetic model is expressed in Eq. (9):

$$q_e = ENTITYNOTDEFINED!!! + \beta \text{Ln}t \tag{9}$$

Where ENTITY NOT DEFINED !!! and β are are Elovic constants obtained from slope and intercept of q_e versus Lnt.

2.9. Goodness of fit model

This model was used to quantitatively compare the applicability of isotherm and kinetic equations [7,30]. The best of fit model was calculated by correlation coefficient (R^2) and Chi-square (X^2) analysis [7,31,32]. The correlation factor was determined from the graphical plots of isotherm and kinetic models while the Chi square test (X^2) was calculated using Eq. (10):

$$\chi 2 = \Sigma \frac{(Qexp - Qcal)^2}{Qcal} \tag{10}$$

Where Q_{exp} is the experimental amount of metal concentration at equilibrium and Q_{cal} is calculated amount of metal concentration at equilibrium. The interpretation of the best fit is thus; the higher the correlation coefficient, the better the fit of model while the lower the chi squared value, the better the fit.

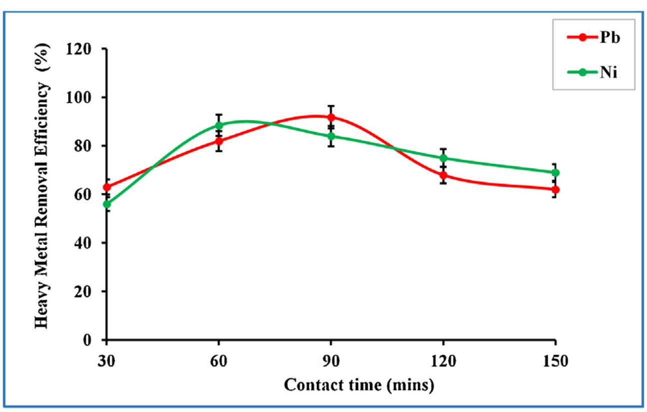

(a): Effect of contact time on heavy metal removal by SCB

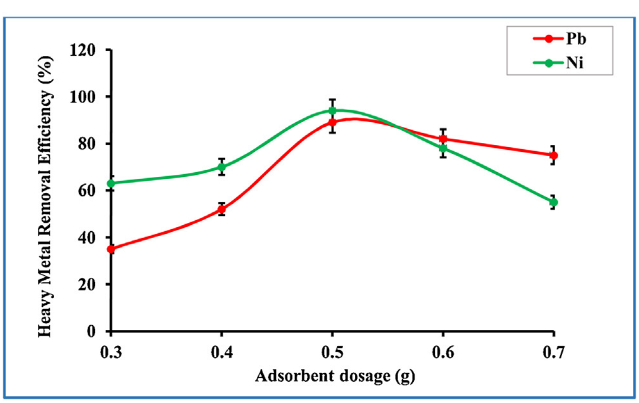

(b): Effect of adsorbent dosage on heavy metal removal by SCB

Fig. 2. Effect of contact time and adsorbent dosage on adsorption of lead and nickel.
(a): Removal efficiency metal ions adsorbed by SCB.
(b): Quantity of metal ions adsorbed by SCB.

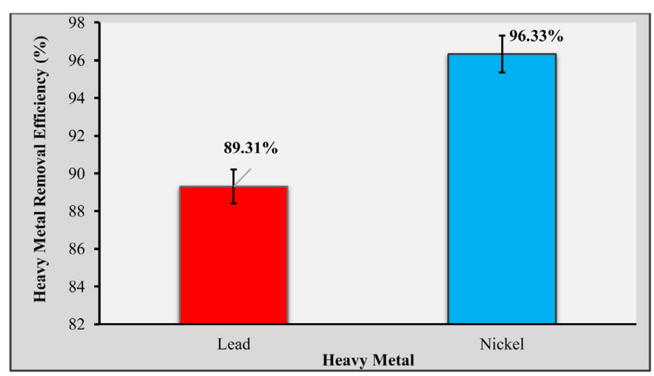

(a): Removal efficiency metal ions adsorbed by SCB

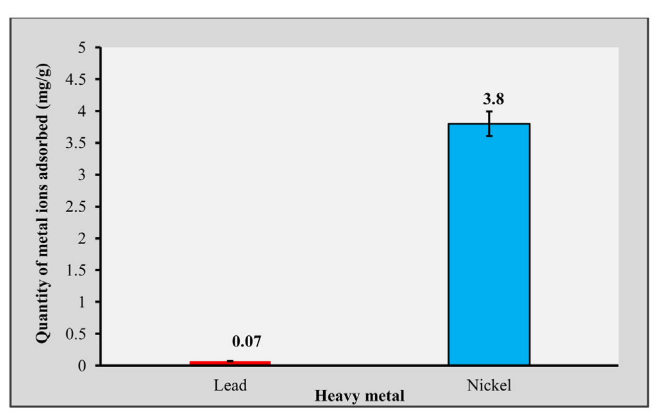

(b): Quantity of metal ions adsorbed by SCB

Fig. 3. Removal efficiency and quantity of metal ions adsorbed by Sugarcane bagasse.

2.10. Desorption of heavy metal ions from metal loaded adsorbents

Reusability of the adsorbent was tested following reported procedures, with the aim of desorbing the metals and restore the adsorbent for effective re-use [33–354]. Desorption experiments were performed by mixing one gram (1 g) of the metal-loaded adsorbent with 100 mL of desorbing agents (0.1 N HNO_3, HCl and NaOH) for 1 h in a rotatory shaker (150 rpm). The amount of metal ions after filtration was determined by atomic absorption spectrophotometer. The percentage desorption efficiency was calculated using Eq. (11):

$$Desorption\ Efficiency\ (\%) = \frac{Amount\ of\ metal\ ion\ desorbed}{Amount\ of\ metal\ ions\ adsorbed} x100 \tag{11}$$

3. Results and discussions

3.1. Physicochemical properties of the untreated waste water

The physicochemical characteristics of the untreated refinery wastewater are presented in Table 1. The wastewater at the time of collection had an average pH of 8.2 and temperature of 26.3 °C which were within the limits set by the Federal Ministry of Environment, Nigeria (FMENV). Temperature and pH are vital factors in determining wastewater quality. Temperature controls the solubility of salts and gases while changes in pH control the biological activities and chemical reactions in aquatic environment [23]. Values recorded for other physicochemical parameters such as turbidity (433 mg/L), dissolved oxygen (2.18 mg/L), chemical oxygen demand (166.67 mg/L), biological oxygen demand (145.3 mg/L), nitrate (92.50 mg/L), sulphate (72.40 mg/L) and phosphate (63.20 mg/L), electrical conductivity (895.33 mg/L), oil and grease (1025 mg/L), were higher than values stipulated by FMENV (Table 1). This observation could be due to the presence of suspended or decaying organic and inorganic compounds which indicates harmful effect to the environment and aquatic life [23,36]. The COD value was found to be larger than the BOD values implying that the organic compounds in wastewater are slowly biodegradable [17].

Heavy metal (lead and nickel) contents of the untreated effluent were many times higher than the recommended limits of FMENV (Table 1). For instance the mean concentrations of lead (0.80 mg/L) and nickel (39.41 mg/L) were found to be 16 and 563 times higher than the recommended limit. Metals are distinctive among pollutants which cause adverse health effect to humans and animals. Irrespective of how metals are used in industrial processes, agriculture or consumer products, some level of human life exposure is unavoidable [15]. The high amounts of heavy metals observed in this study are capable of causing high corresponding increase in the receiving water-bodies thereby affecting human and aquatic life that directly depends on it [37].

3.2. Optimization studies

Experimental parameters are considered important in biosorption of heavy metals. They strongly influence carbon availability, metal solubility, enhance adsorbent performance [15].

3.2.1. Effect of pH and temperature

Heavy metal removal efficiencies against pH and temperature are shown in Fig. 1a and b. The pH of an aqueous solution is a vital factor in the biosorption of metal ions. It determines the surface properties of the adsorbent in terms of surface charges, ionization of the functional groups and degree of dissociation of functional groups present on active sites of adsorbents [38].

The maximum adsorption of Pb (91.3 %) and Ni (88.1 %) occurred at optimum pH of 6 (Fig. 1a). As the pH of the waste water was increased from 4 to 6, the adsorption of lead and nickel increases. This may be due to decrease in competition between metal ions and hydroxonium ions (H_3O) in the waste water [39] and formation of oxides of lead and nickel [40]. These results also agree with many adsorption studies which report pH range of 4–6 as the optimum pH for most metal adsorption by several adsorbents [38,39,62]. This may be due to the excess amounts of OH^- ions present within the solution [4].

The biosorption efficiency of SCB decreased with increase in temperature from 30 °C to 70 °C (Fig. 1b). Maximum removal of Pb and Ni were found to be 89.3 % and 86 % respectively at a temperature of 30 °C. Temperature is an important factor in the biosorption process. The results obtained indicate that temperature of 30 °C was sufficient for complete removal of Pb (II) and Ni (II). The decrease in the adsorption may be due to weak electrostatic interactions between the metal ions and adsorbent at increased temperature [2,4,63]. In addition, the adsorption process of metal ions from aqueous solution can be affected by solution temperature in two ways depending on heat emitted or absorbed. The increasing temperature causes the increase of the adsorption rate for endothermic adsorption while causing the decrease of the adsorption rate for exothermic adsorption [2].

3.2.2. Effect of contact time and adsorbent dosage

Metal removal efficiencies against contact time and adsorbent dosage are shown in Fig. 2a and Fig. 2b. The effect of contact time was determined by monitoring the uptake of the Pb (II) and Ni (II) ions over a period of 150 min at room temperature. For both metals, percentage metal removal reached a maximum within 90 min, after which there was no considerable change (Fig. 2a). The rapid removal efficiency during the first 90 min could be attributed to availability of free active sites at the adsorbent surfaces gradually occupied with time by metal ions [2]. As the binding sites became exhausted, the uptake rate slowed down due to competition for decreasing availability of actives sites by metal ions [35,39,41]. In addition, Kumar et al. [26] also reported that increase in removal efficiency at increased contact time was as a result of reduced boundary layer resistance to mass transfer surrounding the sorbent particles.

The biosorption efficiency of SCB (Fig. 2b) increased with increase in adsorbent dosage from 0.3 to 0.5 g. This could be due to an increase in the number of active sites available for metal adsorption [42,43]. Further increase in adsorbent dosage had no significant increase in metal removal efficiency. This is ascribed to the fact that higher adsorbent dosage provides more active sites which may remain unused during the sequestration reaction [37,41]. It may also be due to overlapping of adsorption sites as a result of overloading of the adsorption site [39,42].

3.3. Heavy metal removal studies

Heavy metal removal efficiency of SCB (Fig. 3a) revealed that 89.31 % and 96.33 % of lead and nickel were removed from the untreated wastewater respectively while the quantities of metal adsorbed by SCB per unit gram were 0.07 and 3.8 mg/g for Pb (II) and Ni (II) respectively (Fig. 3b). The removal efficiency of Ni (II) was greater than Pb (II) because the nickel ions had higher affinity towards the adsorbent [44]. This may be due to differences in molecular mass, ion charges, ionic radius, hydration energy, and electrostatic forces of the metal ions [8,64].

Table 2
Comparison of maximum sorption capacity (mg/g) of test metals onto different adsorbents.

Adsorbents	pH	Maximum adsorption capacity(mg/g)		References
		Pb(II)	Ni (II)	
Sugarcane bagasse	6.0	1.61	123.46	This work
Sugarcane bagasse biochar	5.0	12.74	–	[38]
sugarcane bagasse- derived $ZnCl_2$-activated carbon	6.0	19.3	2.99	[10]
Digested sugarcane bagasse biochar	5.0	135.40	–	[69]
Raw sugarcane bagasse biochar	5.0	81.90	–	[69]
Sugarcane bagasse	6.0	–	2.0	[68]
Acrylic-modified Sugarcane Bagasse	6.0	700	–	[45]
Bamboo stem	5.0	27.95	–	[46]
Magnetite dowex resin nanocomposite	5.5	380	384.0	[16]
Activated carbon from wine making waste	4	38	–	[47]
Lignocellulose/Montmorillonite nanocomposite	6.8	–	94.86	[7]
Date seed biochar	6.0	74.60	–	[35]
Brewed tea waste		1.197	1.163	[48]
Olive stone waste	6.5	–	54.24	[49]

Table 3
FTIR Characteristics of sugarcane bagasse before and metal uptake.

Wavelength range (cm^{-1})	Before uptake	After uptake	Differences in shifts	Assignment
3500–3000	3339.70	3324.80	−14.90	—OH hydroxyl group
2900–2800	2888.70	2899.90	+11.20	—C—H stretching
1740–1680	1729.50	1733.20	+3.70	—CO= carbonyl group
1670–1640	1602.80	1636.30	+33.50	—COOC—arboxylic groups
1280–1240	1241.20	1237.70	−3.50	——CO stretching bond
1150–1020	1036.40	1032.50	−3.9	———COC stretching bond

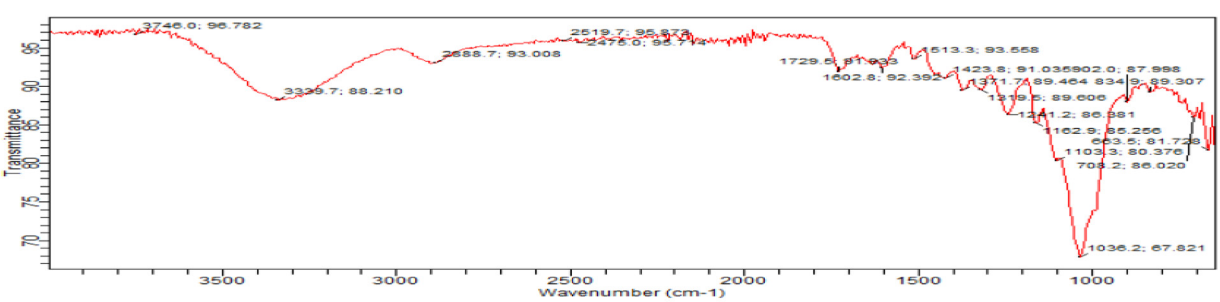

(a) FTIR characteristics of SCB before metal uptake

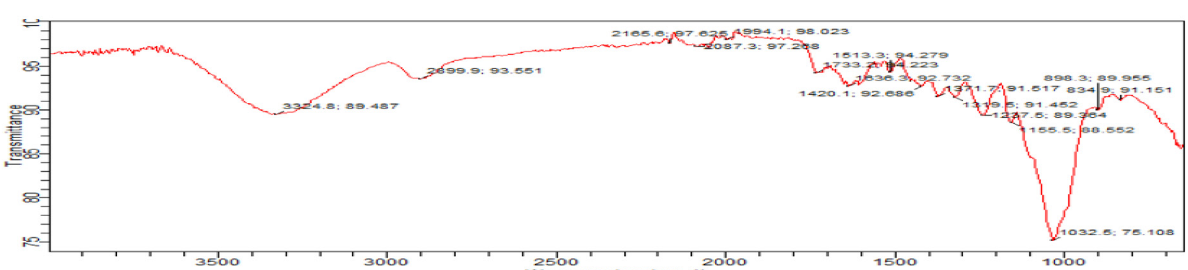

(b) FTIR characteristics of SCB after metal uptake

Fig. 4. FTIR characteristics of SCB before and after metal uptake.

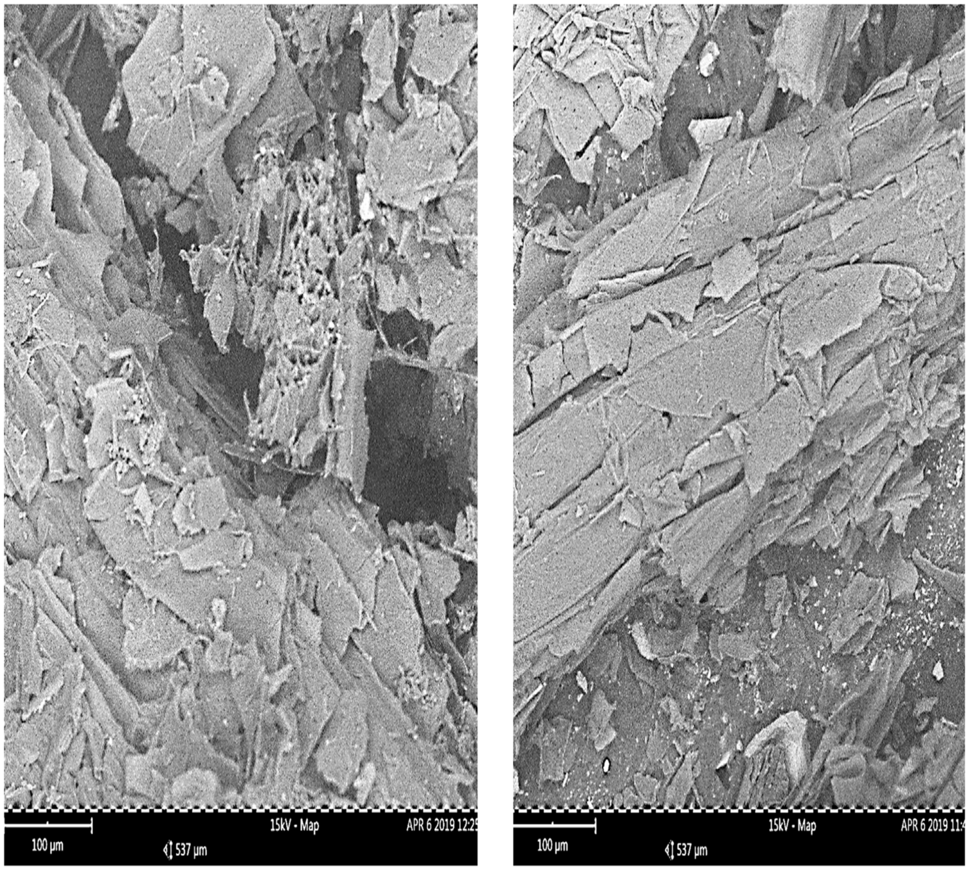

(a) SCB before metal uptake   **(b) SCB after metal uptake**

Fig. 5. Scanning electron images of SCB before and after metal uptake.

Although the ionic radius of Pb (II) and Ni (II) are 133 pm and 83 pm respectively, the lower removal efficiency of Pb (II) may be due to generation of repulsive forces between the metal ions and surface of the sorbent; competition between the metal ions and other ions present in the untreated effluent [8]. Previous works of various researchers on metal removal by other cost effective adsorbents are presented in Table 2.

3.4. Characterization of the adsorbent before and after metal uptake

3.4.1. FTIR

The FTIR spectra of SCB before and after metal sorption were studied to determine the functional groups of the adsorbent (Fig. 5 and Table 3). The infrared (IR) spectrum obtained from FTIR of the SCB (Fig. 4a and b) displayed a number of different absorption peaks (Table 3). The adsorption peaks around 3339.7 and 3324.8 cm^{-1} indicates the existence of —OH hydroxyl groups [50,51]. The peaks at 2888.7 and 2899.9 cm^{-1} are as a result of stretching vibration of C—H which indicate the presence of alkane functional group [65]. The peaks at 1729.5 and 1733.2 cm^{-1} correspond to -C = O stretching carbonyl groups which may be attributed to the hemicelluloses and lignin aromatic group [52]. Bands around 1602.8 and 1636.3 cm^{-1} correspond to -COO-carboxylic acid groups [52]. The bands observed at 1241.2 and 1237 cm^{-1} were assigned to CO—— stretching groups ([50,66]. Bands at 1036.4–1032.5 cm^{-1} were assigned COC——— stretching groups [51,52]. Hence, the major functional groups that took part in adsorption of Pb (II) and Ni (II) were —OH, CH, CO, COC, COOH and CO——=———————. These functional groups originated from compounds such as phenols, aldehydes, ether, lignin aromatic compounds, and ketones (derived from cellulose, hemicellulose and lignin) [53,54]. The shift in the IR spectra may be due to the binding interaction between the metal ion and carbon atom resulting in the formation of metal complex [38,54,43]. Furthermore [45], also revealed that complexation interactions, between metal ions and functional groups on adsorbent surface are the main driving force for adsorption mechanisms.

3.4.2. Scanning electron microscopy

Scanning electron microscopy was conducted for SCB before and after metal uptake to examine the surface morphology for any changes that could occur due to metal uptake (Fig. 5a-b). The surface morphology revealed that SCB before metal uptake had larger pore sizes (Fig. 5a) than the sugarcane bagasse after metal uptake with few pores (Fig. 5b). This might be because the pores were occupied by the metals and other generated small complex compounds [55,45].

3.5. Adsorption isotherms and kinetics

The experimental data were fitted into the selected isotherms and kinetics models used in this study. In each case, the best model considered was one with the highest correlation coefficient (R^2) and lowest chi square (χ^2) values. The closer the R^2 values are to unity (1), the better the goodness of fit and the lower the χ^2 values, the better the fit [30].

3.5.1. Adsorption isotherms

The determined isotherm parameters, correlation coefficients (R^2) and chi square (χ^2) values for adsorption isotherms (Table 4)

Table 4
Adsorption isotherms and kinetic parameters for Pb and Ni uptake by SCB.

Linear Regression of Adsorption Models	Parameters	Pb	Ni
1. Adsorption Isotherm models			
a. Langmuir	q_{max} (mg/g)	1.61	12.35
	K_L (L/mg)	-2.34×10^{-2}	-8.0×10^{-5}
	R_L	1.032	1.033
	R^2	0.9819	0.9650
	χ^2	26.79	284.6
b Freundlich	n	2.3050	5.8928
	K_f (mg g^{-1}) (Lmg^{-1})	1.3766	224.49
	R^2	0.9401	0.8591
	χ^2	16.88	27.2
c. Temkin	B_T (kJmol^{-1})	−2101.4	−86.86
	K_T (Lmg^{-1})	0.420	-5.0×10^{-3}
	R^2	0.9680	0.9133
	χ^2	70.36	148.6
2. Adsorption kinetic models			
a. Pseudo first order	q_e (mg/g)	2.17	12.94
	K_1 (min^{-1})	−0.3363	−0.0440
	R^2	0.5947	0.8255
	χ^2	8.05	1.51
b. Pseudo second order	q_e (mg/g)	0.51	2.6
	K_2 (min^{-1})	1.95×10^{-2}	1.13×10^{-2}
	R^2	0.9814	0.9830
	χ^2	0.024	0.50
c. Elovich	α (mg g^{-1} min^{-1})	0.723	68.25
	β(gmg^{-1})	909.10	24.75
	R^2	0.8563	0.8968
	χ^2	79.54	231.5

Keys: q_{max}=Maximum monolayer adsorption capacity; K_L=Langmuir constant; K_1= Pseudo first order constant; K_2= Pseudo second order constant; R_L=Separation factor; R^2=Correlation coefficient; χ2 =Chi square; n = Adsorption intensity K_f = Freundlich constant; K_T = Binding energy; B_T = Heat of adsorption; L = litre; mg/g = Milligram per gram; kJmol^{-1} =Kilo joule per mole.

showed that Freundlich isotherm had high and low R^2 and χ^2 compared to Langmuir, and Temkin. Hence, the order of isotherm best fit for removal of lead and nickel by SCB was Freundlich < Temkin < Langmuir.

Freundlich isotherm model provided a better fit for the adsorption of metals by test sorbents than Langmuir and Temkin isotherms. This indicates that the adsorption of Pb (II) and Ni (II) on experimental sorbents followed the heterogeneous and multilayer adsorption on the surface of the adsorbent.

Previous reports have also shown best fit of Freundlich isotherm model in describing experimental data. Examples include: Adsorption of Pb (II), Ni (II), and Zn (II) by granular resin and fibrous adsorbent [56], Ni (II), Cd (II), Cu (II), Zn(II) by biochar amended soil [57], Pb (II) by activated carbon [29], As (III) by magnesite–bentonite clay [58].

The negative values of the Langmuir constants and high chi-square (χ^2) values of Temkin constants reveal the inadequacy of the Langmuir and Temkin isotherm to fit the experimental data. This could be due to increase in ionic radius of the metals, decrease in charge densities and adsorption capacity [24,59].

In addition, the negative values obtained for Temkin constant, B_T (heat energy) suggest that metal uptake by sorbent materials could be an exothermic reaction [38,59].

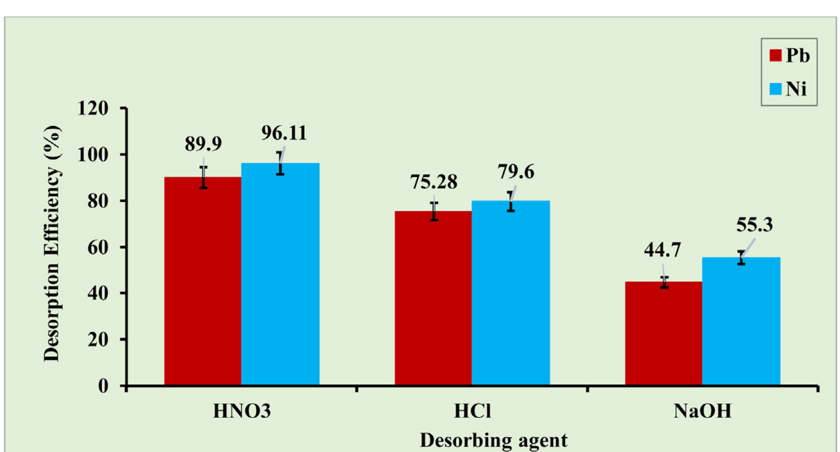

Fig. 6. Metal desorption from metal-loaded sugarcane bagasse.

3.5.2. Adsorption kinetics

The calculated kinetics parameters, correlation coefficients (R^2) and chi square (χ^2) values for pseudo first order, pseudo second order and Elovich models (Table 4) revealed that the data obtained for each of the kinetic models showed a good compliance with the pseudo second-order kinetic model where the correlation coefficient was higher with low chi square value. The order of kinetic model best fit for removal by Pb (II) and Ni (II) was pseudo second order < Elovich < pseudo first order.

The pseudo second order model is based on the assumption that the adsorption of Pb (II) and Ni (II) is govern by chemisorption which also suggests that chemical reactions occurred between the metal ion and the adsorbent, resulting in the formation of strong covalent bonds [28].

The results obtained in this study were in agreement with previous studies, which also reported that the adsorption process followed the pseudo-second-order kinetics [38,60,67]. Adsorption kinetics is an important factor in describing rate of reaction and principal mechanisms involved in adsorption [28].

3.6. Desorption studies

Desorption efficiency for metal elution from SCB by using 0.1 M HNO_3, HCl and NaOH is shown in Fig. 6. The most effective metal stripping agent was HNO_3 which had the highest desorption efficiencies of 89.9 % and 96.11 % for Pb (II) and Ni (II) respectively. This was followed by HCl while the least metal stripping agent was NaOH. Desorption of heavy metals, under acidic conditions causes protonation of the sorbent surface which allows desorption of positively charged metal ions from adsorbent [18]. Some studies in the past have shown high performance of 0.1 M HNO_3 as desorbing agent [26,34,38]. In addition, an effective potential adsorbent for the removal of metal ions must not only have a good adsorption capacity but also a good recovery capacity of metal ions and reusability [33].

4. Conclusion

In the present work, the efficiency of sugarcane bagasse to remove heavy metal ions from untreated refinery effluent was successfully achieved. The optimum conditions for the removal efficiency of Pb (II) and Ni (II) occurred at pH, 6.0; temperature, 30 °C; contact time, 90 min. and adsorbent dosage, 0.5 g. The removal efficiencies of the bagasse were 89.31 % and 96.33 % for Pb (II) and Ni (II) ions respectively. The equilibrium data from the adsorption isotherms were best described by Freundlich isotherm while the adsorption kinetics were best represented by the pseudo-second-order model. The maximum monolayer adsorption capacity of (Pb (II) and Ni (II) were 1.61 mg/g and 123.46 mg/g respectively. Treatment of the metal-loaded sorbents with 0.1 M nitric acid (85.2 %) resulted in higher rate of metal recovery compared to 0.1 M HCl (73.8 %) and NaOH (55.4 %). Therefore, sugarcane bagasse was confirmed to be an effective adsorbent for heavy metal ions with efficient recovery and regeneration performance.

Declaration of Competing Interest

The authors declare that they have no competing financial interests or personal relationships that could have influence the work reported in this paper.

Acknowledgements

The authors would like to thank the staff of the University multipurpose laboratories, Department of Chemistry and Department of Chemical Engineering, Ahmadu Bello University Zaria, Nigeria for all their assistance in heavy metal analysis, sugarcane bagasse characterization and design of experiment analyses.

References

[1] H. Hauwa, C.M.Z. Whong, S.A. Ado, A. Nuhu, Optimization of culture condition for biosorption of lead using Pseudomonas aeruginosa isolated from gold mining site of Anka, Zamfara state, Umaru Musa Yaradua Univ. J. Microbiol. Res. 5 (1) (2020) 43–48.

[2] M.A. Tahoon, S.M. Siddeeg, N.S. Alsaiari, W. Mnif, F.Ben. Rebah, Effective heavy metals removal from water using nanomaterials: a review, Processes 8 (645) (2020) 1–24, doi:http://dx.doi.org/10.3390/pr8060645.

[3] D. Cui, C. Tan, H. Deng, X. Gu, S. Pi, T. Chen, L. Zhou, Biosorption mechanism of aqueous Pb 2 +, Cd 2 +, and Ni 2 + ions on extracellular polymeric substances (EPS), Archaea 2020 (2020) 1–9, doi:http://dx.doi.org/10.1155/2020/8891543 Research.

[4] A.H. El Maghrabi, M.A. Marzouk, M.A. Elbably, M.E.M. Hassouna, Biosorption of manganese by amended Aspergillus versicolor from polluted water sources, Nat. Environ. Pollut. Technol. 9 (4) (2020) 1645–1656.

[5] A. Yulianti, D. Lestari, A. Chafidz, A.R. Hapsari, W. Denly, Magnetically modified corn cob as a new low-cost biosorbent for removal of Cu (II) and Zn (II) from wastewater, J. Bahan Alam Terbarukan 9 (2) (2020) 96–102.

[6] O.K. Moyib, M.A. Ayedun, O.J. Awokoya, O.E. Omotola, Waste printing paper as analogous adsorbents for heavy metals in aqueous solution, Niger. J. Chem. Res. 22 (1) (2017) 29–39. https://www.ajol.info/index.php/njcr/article/view/160397.

[7] L. Zhang, H.A. Loáiciga, M. Xu, C. Du, Y. Du, Kinetics and mechanisms of phosphorus adsorption in soils from diverse ecological zones in the source area of a drinking-water reservoir, Int. J. Environ. Res. Public Health 12 (2015) 14312–14326, doi:http://dx.doi.org/10.3390/ijerph121114312.

[8] J. Hong, J. Xie, S. Mirshahghassemi, J. Lead, Metal (Cd, Cr, Ni, Pb) removal from environmentally relevant waters using polyvinylpyrrolidone-coated magnetite nanoparticles, R. Soc. Chem. Adv. 10 (2020) 3266–3276, doi:http://dx.doi.org/10.1039/c9ra10104g.

[9] A.J. Muñoz, F. Espínola, M. Moya, E. Ruiz, Biosorption of Pb (II) ions by Klebsiella sp. 3S1 Isolated from a wastewater treatment plant: kinetics and mechanisms studies, Biomed. Res. Int. 2015 (2015) 1–12, doi:http://dx.doi.org/10.1155/2015/719060.

[10] T. Tran, Q. Van Thi, P. Bui, T.D. Nguyen, N. Thi, H. Le, L.G. Bach, A comparative study on the removal efficiency of metal ions (Cu2+, Ni2+, and Pb 2+) using sugarcane bagasse- derived ZnCl 2 -activated carbon by the response surface methodology, Adsorpt. Sci. Technol. 35 (1–2) (2017) 72–85, doi:http://dx.doi.org/10.1177/0263617416669152.

[11] J. Aravind, C. Lenin, C. Nancyflavia, P. Rashika, S. S, Response surface methodology optimization of nickel (II) removal using pigeon pea pod biosorbent, Int. J. Environ. Sci. Technol. 12 (2015) 105–114, doi:http://dx.doi.org/10.1007/s13762-013-0391-0.

[12] M. Stevens, B. Batlokwa, Removal of nickel (II) and cobalt (II) from wastewater using vinegar-treated eggshell waste biomass, J. Water Resource Prot. 9 (2017) 931–944, doi:http://dx.doi.org/10.4236/jwarp.2017.98062.

[13] S.H. Abbas, W.H. Ali, Evaluation of biomass type blue cyanophyta algae for the sorption of Cr(III), Zn(II) and Ni(II) from aqueous solution using batch operation system: equilibrium, kinetic and thermodynamic studies, Global Nest J. 20 (1) (2017) 69–82, doi:http://dx.doi.org/10.30955/gnj.002282.

[14] C. Liu, X. Liang, W. Yuan, Desorption of copper ions from the polyamine-functionalized adsorbents: behaviors and mechanisms, Adsorpt. Sci. Technol. 34 (7–8) (2016) 455–468, doi:http://dx.doi.org/10.1177/0263617416663732.

[15] Machido, et al., Resistance to some heavy metals among fungal flora of raw refinery effluent, J. Appl. Sci. Environ. Manag. 18 (4) (2014) 623–627, doi:http://dx.doi.org/10.4314/jasem.v18i4.10.

[16] M.R. Lasheen, I.Y. El-sherif, S.T. El-wakeel, Heavy metals removal from aqueous solution using magnetite Dowex 50WX4 resin nanocomposite, J. Mater. Environ. Sci. 8 (2) (2017) 503–511. http://www.jmaterenvironsci.com/.

[17] U. Pathak, P. Das, P. Banerjee, S. Datta, Treatment of wastewater from a dairy industry using rice husk as adsorbent: treatment efficiency, isotherm, thermodynamics, and kinetics modelling, J. Ermodyn. 2016 (3746316) (2016) 1–7, doi:http://dx.doi.org/10.1155/2016/3746316.

[18] I. Morosanu, C. Teodosiu, C. Paduraru, D. Ibanescu, L. Tofan, Biosorption of lead ions from aqueous effluents by rapeseed biomass, N. Biotechnol. 39 (2017) (2017) 110–124, doi:http://dx.doi.org/10.1016/j.nbt.2016.08.002.

[19] R. Kamari, A.A.A. Shamsudin, S.N.M. Eljiedi, S.T.S. Yusoff, S. Wong, J. Ishak, M.M. A. Jumadi, S. K, Treatment of electronics industry effluent using low-cost and commercial adsorbents: a comparative study treatment of electronics industry effluent using low-cost and commercial adsorbents: a comparative study, J. Phys. Conf. Ser. Paper 1397 (012022) (2019) 1–9, doi:http://dx.doi.org/10.1088/1742-6596/1397/1/012022.

[20] S.A.A. El-gawad, H.M.A. El-aziz, Effective removal of chemical oxygen demand and phosphates from aqueous medium using entrapped activated carbon in alginate, Moj Biol. Med. 3 (6) (2018) 227–236, doi:http://dx.doi.org/10.15406/mojbm.2018.03.00104.

[21] R.M. Hlihor, M. Diaconu, F. Leon, S. Curteanu, T. Tavares, M. Gavrilescu, Experimental analysis and mathematical prediction of Cd (II) removal by biosorption using support vector machines and genetic algorithms, N. Biotechnol. 32 (3) (2015) 358–368, doi:http://dx.doi.org/10.1016/j.nbt.2014.08.003.

[22] E. Ajenifuja, J.A. Ajao, E.O.B. Ajayi, Adsorption isotherm studies of Cu (II) and Co (II) in high concentration aqueous solutions on photocatalytically modified diatomaceous ceramic adsorbents, Appl. Water Sci. 7 (7) (2017) 3793–3801, doi:http://dx.doi.org/10.1007/s13201-017-0527-3.
[23] K.G. Akpomie, F.A. Dawodu, Treatment of an automobile effluent from heavy metals contamination by an eco-friendly montmorillonite, J. Adv. Res. 6 (6) (2014) 1003–1013, doi:http://dx.doi.org/10.1016/j.jare.2014.12.004.
[24] N.T. Abdel-ghani, G.A. El-chaghaby, Biosorption for metal ions removal from aqueous solutions: a review of a review of recent studies, Int. J. Latest Res. Sci. Technol. 3 (1) (2014) 24–42. http://www.mnkjournals.com/ijlrst.htm.
[25] T.M. Elmorsi, Z.H. Mohamed, W. Shopak, A.M. Ismaiel, Kinetic and equilibrium isotherms studies of adsorption of Pb(II) from water onto natural adsorbent, J. Environ. Prot. 05 (17) (2014) 1667–1681, doi:http://dx.doi.org/10.4236/jep.2014.517157.
[26] M. Kumar, A. Kumar, S. Mohd, Study of sorption and desorption of Cd (II) from aqueous solution using isolated green algae Chlorella vulgaris, Appl. Water Sci. 8 (8) (2018) 1–11, doi:http://dx.doi.org/10.1007/s13201-018-0871-y.
[27] K. Naoki, Adsorption of heavy metal onto the materials prepared by biomass, in: Jacob-Lopes Eduardo, Leila Queiroz Zepka (Eds.), Biomass Production and Uses, Intech Open, 2015, pp. 27, doi:http://dx.doi.org/10.5772/58664.
[28] O.C. Izinyon, O.E. Nwosu, L.O. Akhigbe, I.R. Ilaboya, Performance evaluation of Fe (III) adsorption onto brewers' spent grain, Niger. J. Technol. 35 (4) (2016) 970–978, doi:http://dx.doi.org/10.4314/njt.v35i4.36.
[29] A.S. Thajeel, Modeling and optimization of adsorption of heavy metal ions onto local activated carbon, Aquat. Sci. Technol. 1 (2) (2013) 108–134, doi:http://dx.doi.org/10.5296/ast.v1i2.3890.
[30] S. Rahman, K.V. Sathasivam, Heavy metal adsorption onto kappaphycus sp. from aqueous solutions: the use of error functions for validation of isotherm and kinetics models, Biomed Res. Int. 2015 (2015) 1–13, doi:http://dx.doi.org/10.1155/2015/126298.
[31] S. Ananta, B. Saumen, V. Vijay, Adsorption isotherm, thermodynamic and kinetic study of arsenic (III) on Iron oxide coated granular activated charcoal, Int. Res. J. Environ. Sci. Int. Sci. Congress Assoc. 4 (1) (2015) 64–77. www.isca.me.
[32] S. Mondal, K. Aikat, G. Halder, Biosorptive uptake of arsenic (V) by steam activated carbon from mung bean husk: equilibrium, kinetics, thermodynamics and modeling, Appl. Water Sci. 7 (8) (2017) 4479–4495, doi: http://dx.doi.org/10.1007/s13201-017-0596-3.
[33] D. Kołodynska, J. Krukowska, P. Thomas, Comparison of sorption and desorption studies of heavy metal ions from biochar and commercial active carbon, Chem. Eng. J. 307 (2017) 353–363, doi:http://dx.doi.org/10.1016/j.cej.2016.08.088.
[34] S. Benaisa, B. Arhoun, R. El Mail, J.M. Rodriguez-Maroto, Potential of brown algae biomass as new biosorbent of Iron: kinetic, equilibrium and thermodynamic study, J. Mater. Environ. Sci. 9 (7) (2018) 2131–2141. http://www.jmaterenvironsci.com.
[35] Z. Mahdi, Q.J. Yu, A. El, Removal of lead (II) from aqueous solution using date seed - derived biochar: batch and column studies, Appl. Water Sci. 8 (6) (2018) 1–13, doi:http://dx.doi.org/10.1007/s13201-018-0829-0.
[36] T.E. Aniyikaiye, T. Oluseyi, J.O. Odiyo, J.N. Edokpayi, Physico-Chemical Analysis of Wastewater Discharge from Selected Paint Industries in Lagos, Nigeria, Int. J. Environ. Res. Public Health 16 (1235) (2019) 1–17, doi:http://dx.doi.org/10.3390/ijerph16071235.
[37] K.G. Akpomie, F.A. Dawodu, Acid-modified montmorillonite for sorption of heavy metals from automobile effluent, Beni-Suef Univ. J. Basic Appl. Sci. 5 (1) (2016) 1–12, doi:http://dx.doi.org/10.1016/j.bjbas.2016.01.003.
[38] R.G. Poonam, S.K. Bharti, N. Kumar, Kinetic study of lead (Pb 2 +) removal from battery manufacturing wastewater using bagasse biochar as biosorbent, Appl. Water Sci. 8 (4) (2018) 1–13, doi:http://dx.doi.org/10.1007/s13201-018-0765-z.
[39] Z. Kariuki, J. Kiptoo, D. Onyancha, Biosorption studies of lead and copper using rogers mushroom biomass 'Lepiota hystrix', South Afr. J. Chem. Eng. 23 (2017) 62–70, doi:http://dx.doi.org/10.1016/j.sajce.2017.02.001.
[40] J. Kour, P.L. Homagai, M.R. Pokhrel, K.N. Ghimire, Adsorptive Separation of Metal Ions With Surface Modified Desmostachya Bipinnata 13(1), (2012) , pp. 101–106.
[41] M.T. Amin, A.A. Alazba, M.N. Amin, Absorption behaviours of copper, lead, and arsenic in aqueous solution using date palm fibres and orange peel: kinetics and thermodynamics, Polish J. Environ. Stud. 26 (2) (2017) 543–557, doi:http://dx.doi.org/10.15244/pjoes/66963.
[42] H.O. Chukwuemeka-Okorie, P.N. Ekemezie, K.G. Akpomie, C.S. Olikagu, Calcined corncob-kaolinite Combo as new sorbent for sequestration of toxic metal ions from polluted aqua media and desorption, Front. Chem. 6 (273) (2018) 1–13, doi:http://dx.doi.org/10.3389/fchem.2018.00273.
[43] Y. Jin, X. Wang, T. Zang, H. Yang, H. Xiaojing, R. Guangming, X. Xiuhong, Q. Juanjuan, Biosorption of Lead(II) by Arthrobacter sp. 25, Process Optim. Mech. 26 (8) (2016) 1428–1438.
[44] A.A.H. Faisal, Z.A. Al-ridah, L.A. Naji, M. Naushad, H.A. El-serehy, Waste foundry sand as permeable and low permeable barrier for restriction of the propagation of lead and nickel ions in groundwater, J. Chem. 2020 (2020) 1–13, doi:http://dx.doi.org/10.1155/2020/4569176.
[45] W. Kong, J. Ren, S. Wang, Q. Chen, Removal of heavy metals from aqueous solutions using acrylic-modified sugarcane bagasse-based adsorbents: equilibrium and kinetic studies, Bioresources 9 (2) (2014) 3184–3196.
[46] O.J. Akinyeye, T.B. Ibigbami, O.O. Odeja, O.M. Sosanolu, Evaluation of kinetics and equilibrium studies of biosorption potentials of bamboo stem biomass for removal of Lead (II) and Cadmium (II) ions from aqueous solution, Afr. J. Pure Appl. Chem. 14 (June) (2020) 24–41, doi:http://dx.doi.org/10.5897/AJPAC2019.0812.
[47] F. Jose, L. Alcaraz, I. Garc, L. Antonio, Removal of Pb 2 + in wastewater via adsorption onto an activated carbon produced from winemaking waste, Metals 8 (697) (2018) 1–15, doi:http://dx.doi.org/10.3390/met8090697.
[48] H. Çelebi, G. Gök, O. Gök, Adsorption capability of brewed tea waste in waters containing toxic lead (II), cadmium (II), nickel (II), and zinc (II) heavy metal ions, Sci. Rep. Ii (2020) 1–12, doi:http://dx.doi.org/10.1038/s41598-020-74553-4.
[49] Corral Bobadilla Marina, F.S.G. Ruben Lostado Lorza, R. E. G, Adsorptive of nickel in wastewater by olive stone waste: optimization through multi-response surface methodology using desirability functions, Water 12 (1320) (2020) 1–19, doi:http://dx.doi.org/10.3390/w12051320.
[50] Reza Davarnejad, Mostafa Keshavarz, M.H. Moraveji, Integral technique for evaluation and optimization of Ni (II) ions adsorption onto regenerated cellulose using response surface methodology, Arab. J. Chem. 11 (3) (2018) 370–379, doi:http://dx.doi.org/10.1016/j.arabjc.2015.05.022.
[51] S.S. Hussien, O.A. Desouky, S.E. Mohamady, Study on leaching and biosorption processes of some economic, Adv. Environ. Stud. 3 (1) (2019) 179–190, doi: http://dx.doi.org/10.36959/742/215.
[52] K. Attar, H. Demey, D. Bouazza, A.M. Sastre, Sorption and desorption studies of Pb(II) and Ni(II) from aqueous solutions by a new composite based on alginate and magadiite materials keltoum, Polymer 11 (340) (2019) 1–18, doi:http://dx.doi.org/10.3390/polym11020340.
[53] A.I. Anukam, S.N. Mamphweli, P. Reddy, O.O. Okoh, Characterization and the effect of lignocellulosic biomass value addition on gasification efficiency, Energy Explor. Exploit. 34 (6) (2016) 865–880, doi:http://dx.doi.org/10.1177/0144598716665010.
[54] A.A. Guilherme, P.V.F. Dantas, E.S. Santos, F.A.N. Fernandes, G.R. Macedo, Evaluation of composition, characterization and enzymatic hydrolysis of pretreated sugar cane bagasse, Braz. J. Chem. Eng. 32 (1) (2015) 23–33, doi: http://dx.doi.org/10.1590/0104-6632.20150321s00003146.
[55] V.N. Castaldelli, J.L. Akasaki, J.L.P. Melges, M.M. Tashima, L. Soriano, M.V. Borrachero, J. Monzó, J. Payá, Use of slag/sugar cane bagasse ash (SCBA) blends in the production of alkali-activated materials, Materials 6 (2013) 3108–3127, doi:http://dx.doi.org/10.3390/ma6083108.
[56] M.B. Hamdzah, Removal Efficiency for Heavy Metals Ions with Granular Resin and Fibrous Adsorbent, Universiti Teknologi Malaysia, 2018. https://www.semanticscholar.org/paper/Removal-efficiency-for-heavy-metals-ions-with-resin-Hamdzah/02d9584c7cc775811e5e25974cd0318ec82cc856.
[57] A. Bogusz, P. Oleszczuk, R. Dobrowolski, Adsorption and desorption of heavy metals by the sewage sludge and biochar-amended soil, Environ. Geochem. Health 41 (4) (2019) 1663–1674, doi:http://dx.doi.org/10.1007/s10653-017-0036-1.
[58] V. Masindi, M.W. Gitari, H. Tutu, M. De, Application of magnesite – bentonite clay composite as an alternative technology for removal of arsenic from industrial effluents, Toxicol. Environ. Chem. 96 (10) (2014) 1435–1451, doi: http://dx.doi.org/10.1080/02772248.2014.966714.
[59] M. Alshabanat, G. Alsenani, R. Almufarij, Removal of crystal violet dye from aqueous solutions onto date palm Fiber by adsorption technique, J. Chem. (2013) 1–7, doi:http://dx.doi.org/10.1155/2013/210239.
[60] X. Zhao, B. Jia, Q. Sun, G. Jiao, L. Liu, D. She, Removal of Cr 6 ions from water by electrosorption on modified activated carbon fibre felt, R. Soc. Open Sci. 5 (180472) (2018) 1–13.
[61] Teboho, M.C., Mochane, M.J., Motaung, T.E. Linganiso, L.Z., Thekisoe, O.M. and Songca, S.P. (2019). Sugarcane Bagasse and Cellulose Polymer Composites https://www.intechopen.com/chapter/pdf-download/57762 (Date accessed, 2nd August, 2019).
[62] B.A. Ezeonuegbu, D.A. Machido, S.E. Yakubu, Capacity of fungal genera isolated from refinery effluents to remove and bioaccumulate lead, nickel and cadmium from refinery waste, Int. J. Sci. Technol. 3 (6) (2015) 47–52.
[63] A. Kausar, G. MacKinnon, A. Alharthi, J. Hargreaves, H.N. Bhatti, M. Iqbal, A green approach for the removal of Sr(II) from aqueous media: kinetics, isotherms and thermodynamic studies, J. Mol. Liq. 257 (2018) 164–172, doi: http://dx.doi.org/10.1016/j.molliq.2018.02.101.
[64] J.r.m.F. Duval, R.M. Town, H.P. Van Leeuwen, Lability of nanoparticulate metal complexes at a macroscopic metal responsive (bio) interface: expression and asymptotic scaling laws, J. Phys. Chem. C 122 (2018) 6052–6065.
[65] S. Kamsonlian, C. Balomajumder, S. Chand, S. Suresh, Biosorption of Cd (II) and As (III) ions from aqueous solution by tea waste biomass, Afr. J. Environ. Sci. Technol. 5 (1) (2011) 1–7.
[66] C.E. Chigbundu, I. Babayemi, J. Olajiire, C.P. Egbanu, Bio-adsorption of heavy metal ions from aqueous solution using Uziza (*Piper guineense*) stem: characterization, equilibrium and thermodynamic studies, Singapore J. Sci. Res. 10 (2020) 282, doi:http://dx.doi.org/10.3923/sjsres.2020.282.292.
[67] N.A. Fathy, S.T. El-Wakeel, R.R.A. El-Latif, Biosorption and desorption studies on chromium (VI) by novel biosorbents of raw rutin and rutin resin, J. Environ. Chem. Eng. 3 (2015) 1137–1145.
[68] I. Aloma, M.A. Martín-Lara, I.L. Rodríguez, G. Blazquez, M. Calero, Removal of nickel (II) ions from aqueous solutions by biosorption on sugarcane bagasse, J. Taiwan Inst. Chem. Eng. 43 (2012) 275–281.
[69] M. Inyang, B. Gao, W. Ding, P. Pullammanappallil, A.R. Zimmerman, X. Cao, Enhanced lead sorption by biochar derived from anaerobically digested sugarcane bagasse, Sep. Sci. Technol. 46 (2011) 1950–1956.